THE GEOLOGICAL SOCIETY OF AMERICA®

StraboTools: A Mobile App for Quantifying Fabric in Geology

Allen F. Glazner, *Dept. of Geological Sciences, University of North Carolina, Chapel Hill, North Carolina 27599, USA, afg@unc.edu;*
J. Douglas Walker, *Dept. of Geology, University of Kansas, Lawrence, Kansas 66045, USA*

ABSTRACT

Quantification of field observations is an essential step in making them reproducible and shareable, but field geologists have few tools for quantifying field observations of important features such as foliation intensity, crystal alignment, vesicle elongation, joint intensity, and mineral proportions. Here we describe a mobile app, StraboTools, which offers two ways to rapidly and objectively quantify these variables. The edge fabric tool examines grayscale gradients in a photograph and summarizes them with the edge fabric ellipse. For deformation of a homogeneous material with passive markers, this ellipse tracks the strain ellipse. Edge fabric ellipses can be determined on the outcrop and make quick work (5 seconds) of formerly time-consuming and subjective strain-analysis tasks (e.g., Fry and R_f/ϕ analysis). They are remarkably sensitive to subtle deformations that are difficult to see by eye. The color index tool determines the proportion of any component in the photograph whose grayscale level can be isolated (e.g., dark minerals in a granitic rock, feldspar phenocrysts in a lava, or blue epoxy in a thin section). Estimating proportions by eye has poor precision and accuracy; the color index tool is both accurate and precise if a suitable rock face is available. These tools can be used with photomicrographs and aerial photographs as well as in the field.

INTRODUCTION

The granite outcrop in Figure 1A is clearly deformed, with a nice shear fabric running from lower left to upper right in the photo, and a field geologist could easily measure its orientation with a compass. How strong is the fabric? That is harder to quantify, and the geologist would likely apply an adjective such as "moderate" or "strong" in the field and bring an oriented sample back to the lab for further analysis if desired.

Is the granodiorite in Figure 1B deformed? Most observers would say no, but this image, of an originally isotropic granodiorite, was digitally distorted by flattening in one direction and stretching in the perpendicular direction (pure shear). We venture that few would call this a measurable fabric in the field. Being able to detect and measure such subtle features would greatly aid studies of deformation, flow alignment, and related fabrics.

Is there a pebble imbrication in Figure 1C that gives the local direction of current flow? What is the proportion of dark minerals in Figure 1D? These can be difficult questions to answer, and recently at the outcrop in Figure 1D, several professional geologists gave answers ranging from 5% to 30%. This illustrates how difficult this simple and important measurement can be using the eye alone.

This sort of observation and measurement has occupied much of the field workflow in structural geology, petrology, and sedimentary geology for a century or more. Still, such work can be frustratingly qualitative and incomplete. Quantitative and repeatable measurements are the backbone of much of scientific inquiry, yet field geologists have few tools available for making them on many types of features.

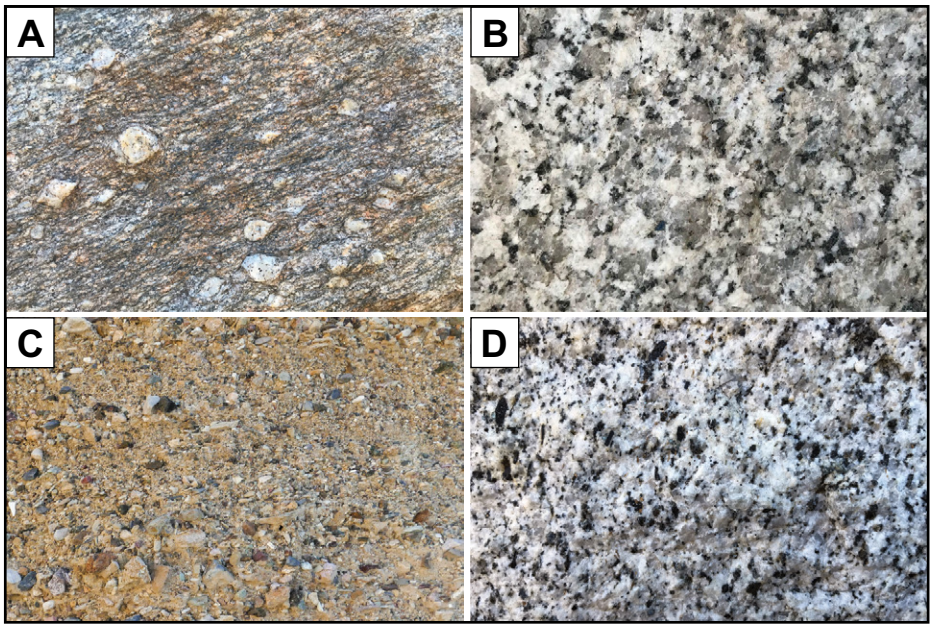

Figure 1. Examples of difficult field problems that can be solved with StraboTools. Answers are in Appendix 1. (A) Deformed granite. The foliation is obvious and easy to measure, but quantifying its strength is difficult to do in the field. (B) Subtly deformed image of a granodiorite outcrop. Do you see a fabric? What deformation was applied? (C) Shadowed outcrop photograph of a cliff in alluvial fan deposits. Is there a pebble imbrication indicating the direction of stream flow? (D) What is the proportion of dark minerals in this granodiorite?

Today, tools available to the field geologist are much the same as they were a century ago: devices for measuring angles, bearings, and distances, and a few categorical measurement aids such as an acid bottle and a magnet. Although mobile phones and laser rangefinders are replacing the compasses and tape measures of yore, the domain of properties that can be measured is largely the same. Field studies are typically the prelude to a comprehensive set of laboratory measurements of chemical composition, porosity, mineral age, mineral or clast preferred orientation, remanent magnetism, and other useful things. Such laboratory studies could be significantly enhanced if some of these properties could be measured in the field. If such measurements could become routine and ubiquitous, then field studies would produce richer results.

It is possible to bring devices into the field to measure chemical composition, magnetic susceptibility, gamma-ray emissions, rock hardness, and other rock properties. These tools are valuable for mapping subtle variations that may be unmappable by eye (e.g., Parkinson, 1996; Aydin et al., 2007; Dühnforth et al., 2010; Coleman et al., 2012), but they are expensive and not widely employed. As a result, aside from orientation measurements, fieldwork is still done in a mostly qualitative or semiquantitative manner, using phrases such as "strong fabric," "coarse-grained," "dark," or "poorly sorted," rather than quantitative measures. For structural analysis, several algorithms have been developed for semiautomated fabric determination from images (e.g., Launeau et al., 1990; Ailleres and Champenois, 1994; Vinta and Srivastava, 2012), but these require processing in the lab.

In this paper, we introduce a mobile app, StraboTools, which allows rapid field measurement and quantification of three quantities: fabric orientation, fabric strength, and the percentage of dark or light minerals in the field of view.

STRABOTOOLS

The StraboTools app provides quantitative data at the outcrop that are otherwise difficult or impossible to estimate in the field or that might be subject to large uncertainty and user-to-user variation. The app was developed for work in plutonic rocks such as granite, but it can be used for fieldwork in any type of rock and for study of thin sections and aerial photographs as well. The analysis uses a photograph taken within the app or imported into it.

The app, currently available for iOS only, comprises two principal tools: edge fabric (EF), for measuring and quantifying preferred orientation, and color index, for determining the percentage of dark minerals. The color index (CI) tool can be used to estimate the abundance of any component that can be separated from others based on grayscale, such as light-colored phenocrysts in a volcanic rock.

THE EDGE FABRIC TOOL

Edge Fabric

Measuring fabrics such as bedding, foliation, and lineation is a large part of geologic fieldwork in structural geology, petrology, and sedimentology. The resulting data (strike and dip or trend and plunge) are quantitative and easily digitized. However, a quantitative assessment of the strength of the fabric is difficult with traditional field tools, and weak fabrics are difficult to reproducibly measure and quantify if they can even be seen at all.

The EF tool provides rapid measurement of preferred shape orientation of grains and can pick up fabrics too subtle to detect by eye alone, such as in Figure 1B. The EF tool works by examining the orientations of grayscale gradients, which are typically particle edges, in the image. To illustrate, Figure 2A shows a 50-by-50 pixel image of two gray stripes and a gray dot. At each pixel, there is a direction of maximum grayscale brightness increase, and its length corresponds to the sharpness of the gradient. These vectors are shown in Figure 2B; blank areas are where the brightness does not vary, and the vectors have length zero. Most of the long brightness vectors point away from the centers of the stripes, and a smaller number point at various other directions. In Figure 2C, all of the vectors from B have been translated to the origin and rescaled. There is a clear concentration perpendicular to the trends of the stripes, which defines the orientation of the long axis of the edge fabric ellipse (EFE; Fig. 2D).

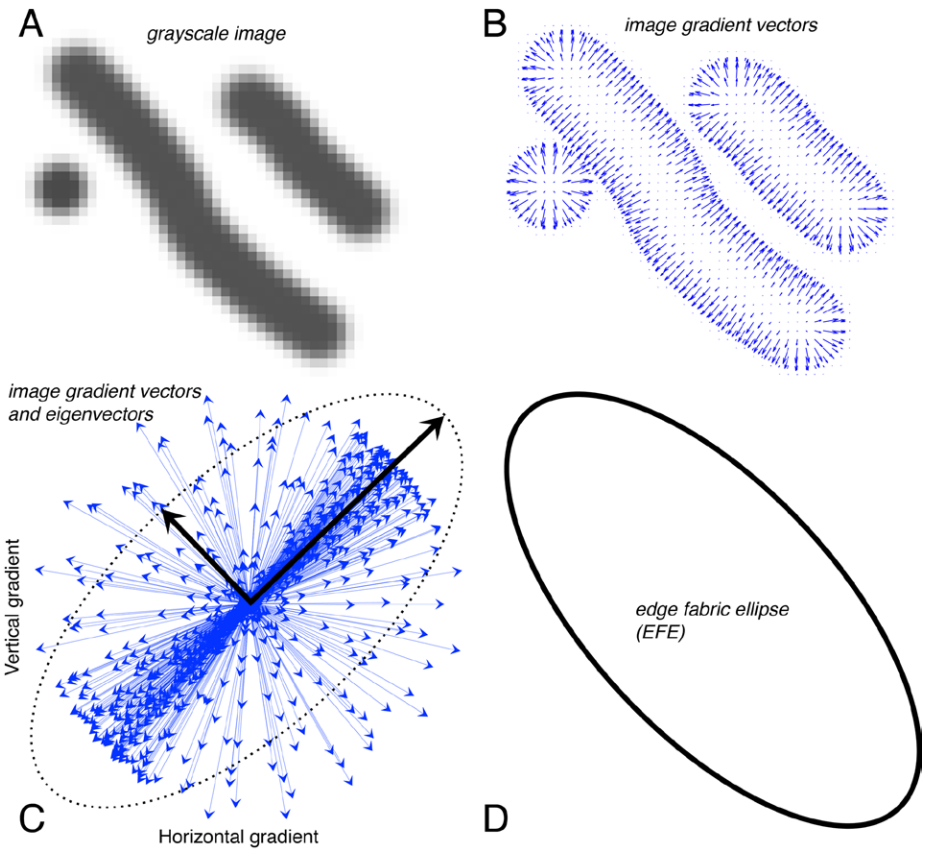

Figure 2. (A) An image of gray stripes 50 pixels on a side. (B) Vectors showing magnitude and direction of the brightness gradient at each pixel. (C) Vectors in B translated to the origin, showing strong grouping perpendicular to dominant edges, along with scaled eigenvectors and ellipse defined by them. (D) Edge fabric ellipse (EFE) derived by rotating ellipse in C 90°.

Axis lengths and orientations are computed using the eigenvectors and eigenvalues of the variance-covariance matrix (Appendix 2). Because the vectors are oriented perpendicular to edges, and we want the dominant edge direction, we simply rotate the ellipse 90° to produce the EFE (Fig. 2D). The aspect ratio of the EFE, designated E, is a measure of the strength of the fabric defined by edge alignment.

The EFE determined from grayscale gradients should be equivalent to the strain ellipse in the case of deformation of a homogeneous material with passive markers. However, empirical tests show that for images deformed digitally by pure shear,

$$E = R^k, \quad (1)$$

where R is the standard strain ratio (ratio of long and short axes of the strain ellipse), and the exponent k typically lies in the range 1.2–1.5 for images of natural samples (e.g., granite or sandstone). Because $k > 1$, the aspect ratio of the EFE, E, is less than that of the strain ellipse, R. This is likely a consequence of image pixelization, and a full treatment of this is beyond the scope of this paper.

Measuring Edge Fabric

To determine EF, the user takes a photograph of a suitable rock face with the mobile device held parallel to the face. The app then calculates the EFE. The tool gives a measure of the fabric's magnitude by reporting the axial ratio E of the ellipse and its orientation by giving the azimuth and trend and plunge of its long axis (Fig. 3). Azimuth is the orientation of the long axis in the plane of the device, and trend and plunge give the orientation of this line in space using the internal magnetometer, gyroscope, and accelerometer of the mobile device to determine its attitude at the time an image is captured. If the feature on the image is produced by, for example, the intersection of foliation with the rock face, then the long axis of the EFE is an intersection lineation that lies in the foliation plane.

Quantifying Strength of Fabric

Fabrics observed in the field can range from mylonites with simple shear strains in the thousands to barely discernible foliations or pebble imbrications. Although the strength of mineral alignment, shape-preferred orientation, and other features can be quantified in the lab, on the outcrop, one is left with qualitative descriptions such as "strong fabric."

The EF tool gives a quantitative measure of fabric strength. In Figure 4, a shear zone comprises various high-strain zones cutting weakly foliated granodiorite. By making EFEs in subareas, a gradation in strength and orientation of fabric is clear. This can be done rapidly on the outcrop.

Making Fabric Measurement Portable and Fast

Perhaps the most commonly used text on quantitative strain analysis is Ramsay and Huber (1983) Sessions 5–8 (pages 73–149). They describe methods and give exercises appropriate to the sorts of rocks discussed here, with the analyses commonly performed using the Fry (1979) center-to-center technique or the R_f/ϕ technique of Dunnet (1969). The former involves finding anticlustered markers and graphing their center-to-center distances; the latter measuring the aspect ratios and elongation directions of elliptical markers, and then finding a finite-strain ellipse that best

Figure 3. Using the edge fabric tool. The mobile device is held parallel to the plane being photographed. The app calculates the edge fabric ellipse and reports its azimuth (long axis of the ellipse, relative to "up" on the screen), its trend and plunge in space, and its axial ratio *E*. Calculations take 5 seconds or less. The analysis can be captured as a screenshot, and the trend and plunge can be copied for pasting into Stereonet Mobile (Allmendinger, 2019). StraboTools locks to landscape display.

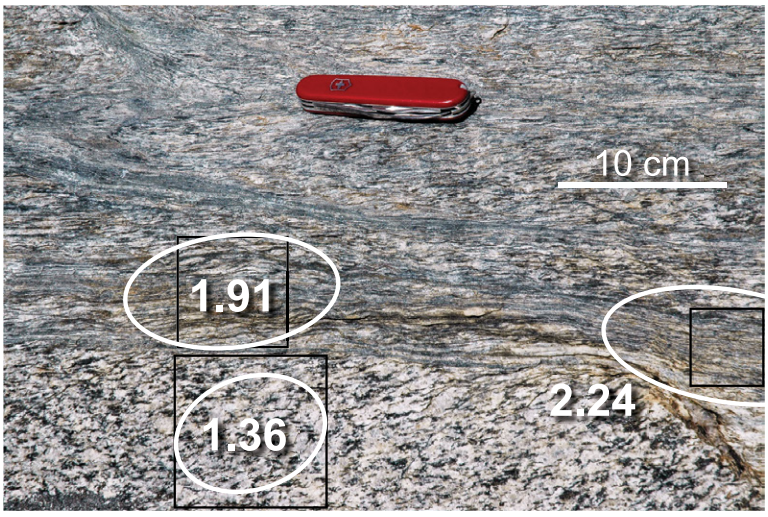

Figure 4. Edge fabric ellipses of three subareas of this shear zone provide field-obtainable, objective measures of fabric intensity and orientation. Shear zone cuts Jurassic granodiorite near Chickenfoot Lake, Sierra Nevada, California, USA.

explains them. Both techniques are labor-intensive and subjective, even with image analysis and automation.

EFEs allow rapid analysis of deformed markers in the field or laboratory. Figures 5A–5D show three artificial examples, and in each case, the EFE determined from StraboTools provides a close estimate of the imposed strain. Figure 5C shows randomly oriented, randomly shaped ellipses, deformed by 10% pure-shear stretching (strain ratio $R = \frac{1.1}{1/1.1} = 1.21$) along an azimuth of 065. The EFE (red) is almost coincident with the imposed strain ellipse (blue), yielding an EFE aspect ratio E of 1.18 and an azimuth of 063. This is a classic subject for R_f/ϕ analysis, but it is difficult to see how one could infer the true deformation (blue star in Fig. 5D) from the scatter of R_f/ϕ points. The EFE solution (red star) again aligns well with the true deformation.

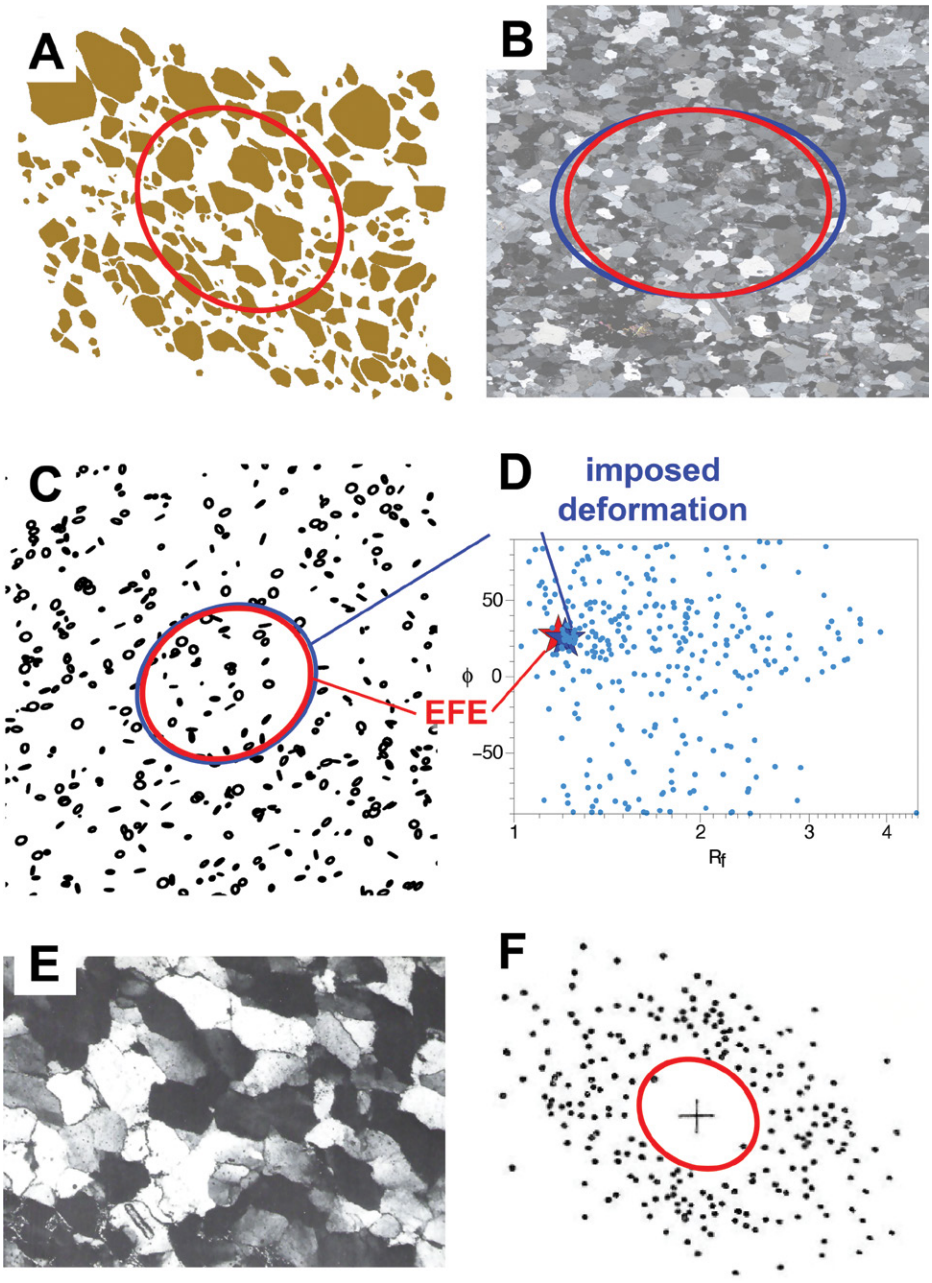

Figure 5. Examples of strain analysis using StraboTools. Red figures are edge fabric ellipses (EFEs) determined with the app, and blue figures are the imposed deformation. (A) Artificial pattern from Waldron et al. (2007), deformed along an undefined axis with strain ratio R = 1.3; the edge fabric tool gives E = 1.21 with an elongation azimuth of 133°. Correcting using Equation 1 with k = 1.3 gives E = 1.28, very close to imposed strain. (B) Cross-polarized thin section view of an isotropic aplite dike deformed by 20% shortening in the vertical direction and 25% stretching in the horizontal (R = 1.56), with EFE (E = 1.41, which corrects with Equation 1–1.56). (C) Ellipses with random axial ratios and orientations that were stretched 10% along an azimuth of 065. Agreement between the imposed strain (blue) and computed EFE (red) strain is excellent. (D) R_f/ϕ plot of data from C, with the imposed deformation and EFE solutions indicated by stars. It is hard to see how one could infer the imposed deformation (blue star) from the scatter of points, but the EFE solution matches it well. (E) Thin section view of deformed quartzite from Ramsay and Huber (1983, p. 118). (F) Their Fry plot derived from it, with EFE. The EFE agrees well with the elliptical void.

Figure 5E is a thin-section view of deformed quartzite from Ramsay and Huber (1983, *their* figure 7.16, p. 118). Their Fry plot is given in Figure 5F along with the EFE. In such a plot, the shape of the hole in the center is an estimate of the strain ellipse. Ramsay and Huber (1983, p. 124) noted, "It is not an easy matter to identify with confidence the dimensions of the elliptical form of the point data," highlighting the subjectivity involved in determining R. The EFE provides a good fit to the Fry plot and is an objective measure of the fabric.

EFEs have utility in other fields as well. At the micro scale they allow measurement of orientation and strength of microlite alignment, vesicle elongation, compaction fabric, and other textural features in thin section. At the macro scale they offer a way to measure and quantify the orientation and frequency of joints, dikes, and other features on aerial photographs. Because of its speed and ease of use, StraboTools makes taking many measurements a practical and efficient reconnaissance exercise.

Caveats

It is important to note that the EFE is simply a measure of the preferred orientation of grayscale gradients in the image. If we take a homogeneous image to start, whether it be a rock or artificial random pattern of circles, E correlates with the distortion we apply to the image, which approximates the finite strain.

Sedimentary compositional or textural banding typically produces EFEs with large Es, but these are not a result of deformation. In thin section, plagioclase twinning, perthitic texture, and other phenomena will generate edge alignments that are unrelated to deformation. In these cases, however, the EFE is still a quantitative measure of edge alignment and fabric in the image. Conversely, many fabric patterns that are obvious to the eye will be invisible to EFE analysis. For example, alternating layers of black and white circles will produce an isotropic EFE, even though layering is quite apparent.

E values are not necessarily equal to the finite strain. As reviewed in Ramsay and Huber (1983), determining finite strain means understanding all of the possible deformation mechanisms (e.g., creep, grain-boundary sliding, etc.). StraboTools does not give this information, but *E* correlates with strain, and the EFE aligns well with fabric, even fabrics that are too subtle to see (Fig. 1). For an igneous rock, the EFE may capture a subtle grain shape fabric or crystal alignment not evident in the field.

There are several cautions about using EFEs. First, they are highly sensitive to shadows and cracks or fractures. In tests on glacially polished outcrops, a low sun angle can produce an elongate EFE whose axis is perpendicular to the sun azimuth even when visible shadows are not apparent. It is good practice to work with evenly shadowed surfaces. Second, although one can snap photos of images from computer screens, many artifacts, such as moiré patterns and the rectangular nature of pixels, can affect the results. High-resolution original images should be used whenever possible.

COLOR INDEX

Color index (CI), the volume percent of dark minerals visible in an outcrop of plutonic rock, is commonly estimated in the field. In granitic rocks, dark minerals such as biotite, hornblende, clinopyroxene, Fe-Ti oxides, and titanite are commonly easy to observe, but estimating their percentage by eye, especially when the percentage is small, is a notoriously difficult endeavor even for experienced observers. Comparison charts (Folk, 1951; Compton, 1985) are helpful, but it is still difficult to estimate CI accurately or precisely by eye, with visual psychology playing a prominent role in introducing biases (Allen, 1956; Dennison and Shea, 1966).

Accurate measurement of CI in the field could allow the delineation of zoning patterns that previously required laboratory or thin-section analysis. For example, the Half Dome and Cathedral Peak plutons in Yosemite National Park form a gradationally nested pair with a consistent inward decrease in CI that accompanies significant parallel changes in bulk composition (Bateman et al., 1988). The Cathedral Peak Granodiorite ranges from CI ~10 and SiO_2 ~68 wt% at its outer contact to CI ~4 and SiO_2 ~72 wt% at its inner. The gradual factor-of-two variation in CI is well within the typical error range of visual CI estimates (see Fig. 1D) and would be difficult to pick up by visual means alone.

The CI tool (Fig. 6) provides a rapid, precise, and accurate tool for estimating CI. In practical use on suitable rock faces, CI is typically reproducible within 1 or 2 absolute percent (e.g., 15 ± 2). The values determined by the CI tool match those determined by point counting within the same range.

FIELD GEOLOGY IN 2020 AND BEYOND

Using StraboTools can significantly enhance the practice of field geology by providing objective ways to collect data types that are impractical or impossible to collect in the field, subject to poor precision, or arduous and time-consuming to do later in the lab. StraboTools lets the field geologist examine rock fabrics in situ or back in the lab with thin sections or cut slabs. Because the app requires the user to capture an image and work on that same picture, it can be used to thoroughly document the data collected and can be reproduced or tested on the same source by other scientists. The tools also record the location and orientation of the image, so it becomes more practical to reproduce the actual field observations at a later date.

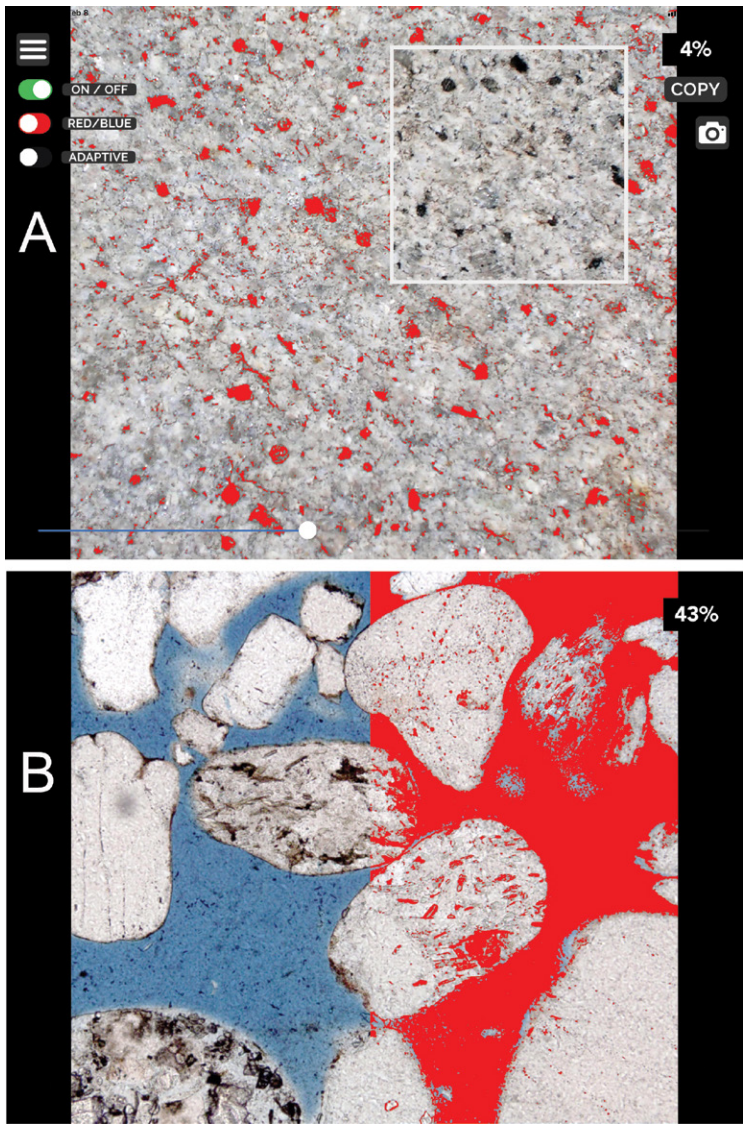

Figure 6. The color index (CI) tool in use. The user takes a photograph of a clean, shadow-free rock face and then uses the slider (lower left) to highlight the desired pixels in red or blue. (A) Determination of CI in a leucocratic granodiorite. The CI is displayed at upper right. A portion of the highlighted pixels has been erased to show the unhighlighted image below. (B) Using the CI tool for quick estimation of the percentage of porosity, as represented by blue epoxy, in a sandstone. The left half of the image is the original photomicrograph; on the right half the slider has been adjusted to highlight the epoxy. Dark inclusions represent ~3% of the image (as determined with the slider); thus, the porosity is 40%. Photomicrograph by Michael C. Rygel.

In his Presidential Address to the Geological Society of America, "New Technology; New Geological Challenges," B.C. Burchfiel (2003 [published in 2004]) made a compelling case that the geological community must embrace new modes of data collecting. At that time, precise GPS measurements were revolutionizing active tectonics and opening entirely new avenues of research. Developing and adopting new mobile technology can advance our ability to perform basic field geology at the individual investigator level. Images and interpretations can be easily shared, discussed, and interpreted by scientists and the interested public. Citizen scientists could have a role in collecting and evaluating geologic data in ways similar to that done for plants and animals with iNaturalist (https://www.inaturalist.org), with over 275,000 species identified, and eBird (https://ebird.org), with more than 100,000,000 bird sightings each year.

SHARING DATA

We envision that StraboTools will lead to more sharing of data and make fieldwork more transparent, reproducible, and searchable. StraboTools was developed as a spinoff of the StraboSpot project, which allows field geologists to collect, store, and share geologic data more easily. StraboSpot is currently focused on collecting general field data for structural geology, petrology, sedimentary geology, and volcanology (Walker et al., 2019). Although not yet a direct part of StraboSpot, StraboTools data and images can be entered into StraboSpot and StereonetMobile (Allmendinger et al., 2017).

SUMMARY

We have developed a mobile app that allows field geologists to make quantitative measurements of features such as foliation orientation and intensity, mineral alignment, and mineral proportions rapidly, precisely, and reproducibly. The app can pick up subtle fabrics (e.g., weak foliation, flow alignment, or pebble imbrication) that can be difficult to see. It allows objective measurement of features that were heretofore subjectively evaluated or just not seen, and can be used to quantify fabrics in photomicrographs and aerial photographs. It rapidly and objectively performs fabric analyses that were formerly time-consuming, subjective, and of low precision.

ACKNOWLEDGMENTS

Jason Ash is a crucial partner in this effort, doing the hard work of turning Matlab code into a stable app. We thank all the participants at various StraboSpot workshops and field trips for their input into how to improve the app. We thank an anonymous reviewer and editor Peter Copeland for reviews that greatly improved the presentation. John Bartley and Kevin Stewart were valuable sounding boards during development, and they and Andreas Möller provided constructive reviews of the manuscript. This work was supported in part by National Science Foundation grants EAR 1639724 to AFG and EAR 1347331, ICER 1639734, and ICER 1639738 to JDW, and by the Mary Lily Kenan Flagler Bingham Professorship at the University of North Carolina.

APPENDIX 1

Puzzle Answers

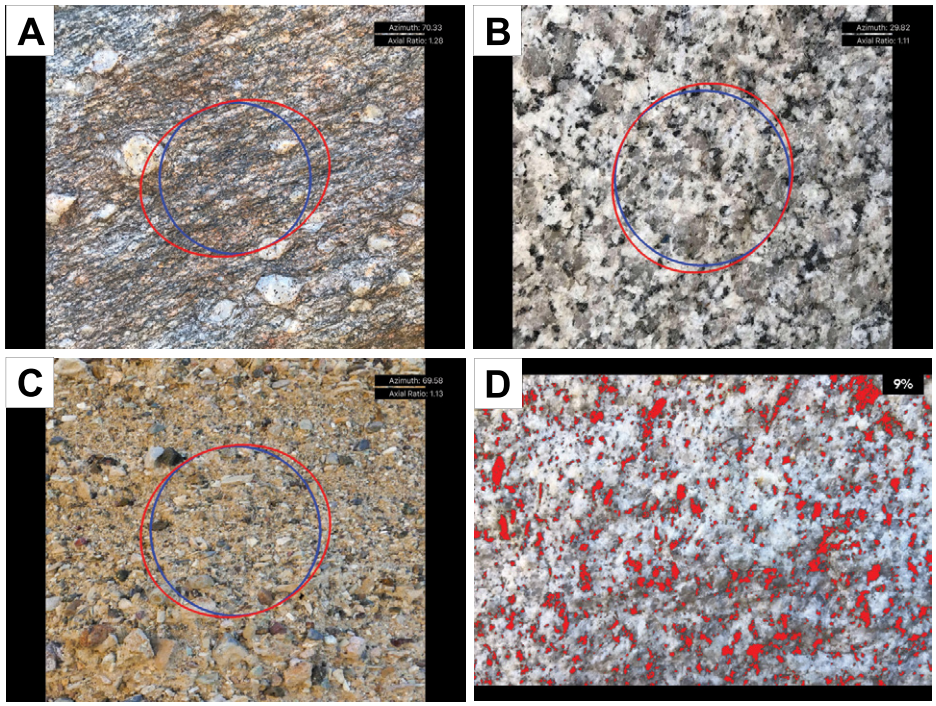

Screenshots of answers to the puzzles in Figure 1. Blue circles are for reference. (A) Foliation in deformed granite (Inyo Range, California, USA) has an edge fabric ellipse (EFE) aspect ratio (*E*) of 1.28 at an azimuth of 070 in the photo. (B) This image of granodiorite (Yosemite National Park, California, USA) was deformed by pure-shear stretch of 10% along a bearing of 030 (*R* = 1.22); EFE gives *E* = 1.11 along 030. (C) Shadowed vertical face cut into alluvial deposits (Death Valley National Park, California, USA), downstream to right, yields an EFE long axis rotated 20° counterclockwise from horizontal. The camera was held with a horizontal horizon, and layering is essentially horizontal, but EFEs in this and several other photos of the same face are consistently aligned with their long axes rotated 20° to 30° counterclockwise from horizontal. We attribute this to pebble imbrication and suggest that EFEs may aid the detection of these subtle fabrics. (D) Color index determination on this granodiorite (Peninsular Ranges, California, USA) yields 9% dark minerals. EFE (not shown) detects the rather obvious steep fabric defined by alignment of the dark minerals. See the original photos in the Supplemental Material.[1]

APPENDIX 2

Calculation of Edge Fabric

At each pixel in an image, there is a direction of maximum grayscale brightness increase. We compute this vector at each point by convolving the grayscale image with a 3-by-3 Sobel kernel (Sobel and Feldman, 1968) to get the horizontal brightness gradient at each pixel, and with the transpose of the kernel to get the vertical gradient. Vectors defined by these two components are shown in Figure 2B.

The StraboTools app downsamples the image to 1000 pixels on the long edge. Hence, a typical image has 10^6 pixels, at each of which there is a horizontal and vertical component of gradient. We form a 2-by-2 variance-covariance matrix from this 10^6-by-2 gradient matrix and calculate its eigenvectors and eigenvalues. These eigenvectors, scaled by the corresponding eigenvalues' square roots, are plotted in Figure 2C along with the ellipse that they define. As the vectors point perpendicular to edges, and we want the dominant edge direction, we rotate the ellipse 90° to produce the EFE (Fig. 2D).

The aspect ratio of the EFE is given by the square root of the ratio of the eigenvalues of the variance-

[1]Supplemental Material. Original photos from Figure 1. Please visit https://doi.org/10.1130/GSAT.S.12429926 to access the supplemental material, and contact editing@geosociety.org with any questions.

covariance matrix. The eigenvalues are the variances of the data projected onto the corresponding eigenvectors; the longer eigenvector is the direction that maximizes this projected variance (Dunteman, 1989, p. 29), and we take square roots to convert to the actual data spread (standard deviation). The aspect ratio is thus the ratio of the data spread in the direction of the longer eigenvector to that in the direction of the shorter eigenvector (Spruyt, 2014).

REFERENCES CITED

Ailleres, L., and Champenois, M., 1994, Refinements to the Fry method (1979) using image processing: Journal of Structural Geology, v. 16, p. 1327–1330, https://doi.org/10.1016/0191-8141(94)90073-6.

Allen, J.E., 1956, Estimation of percentages in thin sections—Considerations in visual psychology: Journal of Sedimentary Petrology, v. 26, p. 160–161, https://doi.org/10.1306/74D704F7-2B21-11D7-8648000102C1865D.

Allmendinger, R., 2019, Stereonet Mobile: version 3.4.1 [mobile application software]: Retrieved from https://apps.apple.com/us/app/stereonet-mobile/id1194772610.

Allmendinger, R.W., Siron, C.R., and Scott, C.P., 2017, Structural data collection with mobile devices: Accuracy, redundancy, and best practices: Journal of Structural Geology, v. 102, p. 98–112, https://doi.org/10.1016/j.jsg.2017.07.011.

Aydin, A., Ferré, E.C., and Aslan, Z., 2007, The magnetic susceptibility of granitic rocks as a proxy for geochemical composition: Example from the Saruhan granitoids, NE Turkey: Tectonophysics, v. 441, p. 85–95, https://doi.org/10.1016/j.tecto.2007.04.009.

Bateman, P.C., Chappell, B.W., Kistler, R.W., Peck, D.L., and Busacca, A.J., 1988, Tuolumne Meadows Quadrangle, California; analytic data: U.S. Geological Survey Bulletin, v. 1819, p. 43.

Burchfiel, B.C., 2004, New technology; new geological challenges: GSA Today, v. 14, p. 4–10, https://doi.org/10.1130/1052-5173(2004)014<0004:NTNGC>2.0.CO;2.

Coleman, D.S., Bartley, J.M., Glazner, A.F., and Pardue, M.J., 2012, Is chemical zonation in plutonic rocks driven by changes in source magma composition or shallow-crustal differentiation?: Geosphere, v. 8, p. 1568–1587, https://doi.org/10.1130/GES00798.1.

Compton, R.R., 1985, Geology in the Field: New York, Wiley, 398 p.

Dennison, J.M., and Shea, J.H., 1966, Reliability of visual estimates of grain abundance: Journal of Sedimentary Petrology, v. 36, p. 81–89, https://doi.org/10.1306/74D71410-2B21-11D7-8648000102C1865D.

Dühnforth, M., Anderson, R.S., Ward, D., and Stock, G.M., 2010, Bedrock fracture control of glacial erosion processes and rates: Geology, v. 38, p. 423–426, https://doi.org/10.1130/G30576.1.

Dunnet, D., 1969, A technique of finite strain analysis using elliptical particles: Tectonophysics, v. 7, p. 117–136, https://doi.org/10.1016/0040-1951(69)90002-X.

Dunteman, G.H., 1989, Principal components analysis (Sage University paper series on quantitative applications in the social sciences, no. 69): London, SAGE, 96 p.

Folk, R.L., 1951, A comparison chart for visual percentage estimation: Journal of Sedimentary Petrology, v. 21, p. 32–33, https://doi.org/10.1306/D4269413-2B26-11D7-8648000102C1865D.

Fry, N., 1979, Random point distributions and strain measurement in rocks: Tectonophysics, v. 60, p. 89–105, https://doi.org/10.1016/0040-1951(79)90135-5.

Launeau, P., Bouchez, J.L., and Benn, K., 1990, Shape preferred orientation of object populations: Automatic analysis of digitized images: Tectonophysics, v. 180, p. 201–211, https://doi.org/10.1016/0040-1951(90)90308-U.

Parkinson, D.N., 1996, Gamma-ray spectrometry as a tool for stratigraphical interpretation: Examples from the western European Lower Jurassic, *in* Hesselbo, S.P., and Parkinson, D.N., eds., Sequence Stratigraphy in British Geology: Geological Society (London) Special Publication 103, p. 231–255, https://doi.org/10.1144/GSL.SP.1996.103.01.13.

Ramsay, J.G., and Huber, M.I., 1983, The Techniques of Modern Structural Geology, Volume 1: Strain Analysis: London, Academic Press, 307 p.

Sobel, I., and Feldman, G., 1968, A 3 × 3 isotropic gradient operator for image processing: A talk at the Stanford Artificial Project in 1968, p. 271–272.

Spruyt, V., 2014, A geometric interpretation of the covariance matrix: https://www.visiondummy.com/2014/04/geometric-interpretation-covariance-matrix/ (accessed 15 Feb. 2020).

Vinta, B.S.S.R., and Srivastava, D.C., 2012, Rapid extraction of central vacancy by image-analysis of Fry plots: Journal of Structural Geology, v. 40, p. 44–53, https://doi.org/10.1016/j.jsg.2012.04.004.

Waldron, J.W.F., and Wallace, K.D., 2007, Objective fitting of ellipses in the centre-to-centre (Fry) method of strain analysis: Journal of Structural Geology, v. 29, p. 1430–1444, https://doi.org/10.1016/j.jsg.2007.06.005.

Walker, J.D., Tikoff, B., Newman, J., Clark, R., Ash, J.M., Good, J., Bunse, E.G., Möller, A., Kahn, M., Williams, R., Michels, Z., Andrew, J.E., and Rufledt, C., 2019, StraboSpot data system for structural geology: Geosphere, v. 15, https://doi.org/10.1130/GES02039.1.

Manuscript received 22 Feb. 2020
Revised manuscript received 19 May 2020
Manuscript accepted 22 May 2020